ELSEVIER

International Journal of Fatigue 21 (1999) S221–S231

International Journal of Fatigue

www.elsevier.com/locate/ijfatigue

Critical issues in high cycle fatigue

T. Nicholas *

US Air Force Research Laboratory, Materials and Manufacturing Directorate, Wright-Patterson AFB, OH 45433-7817, USA

Abstract

High cycle fatigue (HCF) failures in materials used in rotating components of gas turbine engines have often been found to be attributable to fatigue loading on materials which have sustained damage from other sources. Damage can be present in the form of initial material or manufacturing defects, or can develop during service operation. Three major sources of in-service damage have been identified which can alter the HCF resistance individually or in conjunction with one another: low cycle fatigue (LCF), foreign object damage (FOD), and fretting. Methodologies for treating such damage in establishing material allowables are considered. Some recent results on the effects of damage on the Haigh (Goodman) diagram and a discussion of the life management aspects of HCF are presented.

Keywords: High cycle fatigue; Fatigue initiation; Damage tolerance; Turbine engines; Material behavior

1. Introduction

The high incidence of high cycle fatigue (HCF) related failures over the past several years in US Air Force gas turbine engines, combined with the substantial maintenance costs and potential detrimental effects on operational readiness, have led the Air Force to re-evaluate the design and life management procedures for HCF. In attempting to assess the root cause of HCF failures and find methods for reducing the incidence of such failures, the relatively empirical nature of the procedures now in place becomes abundantly clear. Further, the lack of detailed information on vibratory loading and dynamic response of components as well as material capability under HCF, particularly in the presence of initial or in-service damage, makes anything but a highly empirical approach impractical at this time. To address these shortcomings, the US Air Force initiated a National High Cycle Fatigue Program to develop a technology base for implementation of damage tolerance procedures for HCF in gas turbine engines. This paper focuses on the material capability aspects of the damage tolerant approach for design and life management of components subjected to HCF.

2. Damage tolerance

The natural tendency in the implementation of a "damage tolerant" approach to fatigue is to relate remaining life based on predictions of crack propagation rate to inspectable flaw size. In low cycle fatigue (LCF), this has been shown to work well, and such an approach was adapted by the US Air Force in 1984 as part of the ENSIP Specification [1]. For HCF, direct application of such an approach cannot work for "pure" HCF because required inspection sizes are well below the state-of-the-art in non-destructive inspection (NDI) and the number of cycles in HCF is extremely large because of the high frequencies involved. The basic problem is illustrated schematically in Fig. 1 which shows that LCF involves early crack initiation and a long propagation life as a fraction of total life. There is no attempt in this schematic to represent the complex processes in the early stages of crack nucleation and initiation, nor to distinguish between fatigue of smooth bar versus notched samples. In general, LCF cracks are typically of an inspectable size early enough in total life so that there is a considerable fraction of life remaining during which an inspection can be made. HCF, on the other hand, requires a relatively large fraction of life for initiation to an inspectable size, or the creation of damage which can be detected, to occur. This results in a very small fraction of life remaining for propagation. It must be pointed out that considerable research is being conducted

* Corresponding author. Tel.: +1-937-255-1347; fax: +1-937-656-4840.

E-mail address: theodore.nicholas@afrl.af.mil (T. Nicholas)

0142-1123/99/$ - see front matter
PII: S0142-1123(99)00074-2

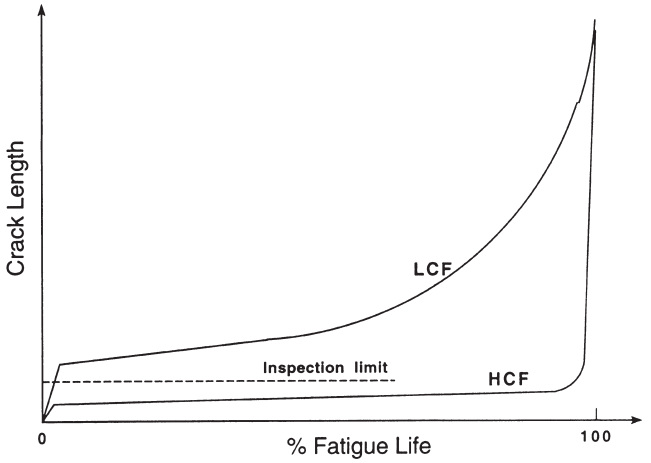

Fig. 1. Schematic showing conceptual differences between HCF and LCF.

at the present time to identify and detect HCF damage in the early stages of total fatigue life.

While a damage tolerant approach may seem out of the question at present for HCF, the most pressing problems in field failures are not related to material capability under pure HCF. Rather, the problems fall into two categories. First, and foremost, is the existence of vibratory stresses from unexpected drivers and structural responses which exceed the material capability as determined from laboratory specimen and sub-component tests. Design allowables are normally obtained on material which is representative of that used in service including all aspects of processing and surface treatment and are often represented as points on a Haigh or "Modified Goodman diagram". (This point is qualified in the following paragraph.) The second category involves the introduction of damage into the material during production or during service usage. The three most common forms of damage, either alone or in combination, are LCF cracking, foreign object damage (FOD), and fretting fatigue. To account for this damage, or to design for pure HCF, the concept of a threshold below which HCF will not occur is necessary because of the potentially large number of HCF cycles which can occur over short service intervals. This is due to the high frequency of many vibrational modes, often extending into the kHz regime. In fact, current design for HCF through the use of a Haigh diagram seeks to identify maximum allowable vibratory stresses so that HCF will not occur in a component during its lifetime. The current ENSIP specification requires this HCF limit to correspond to 10^9 cycles in non-ferrous metals, a number which is hard to achieve in service and even harder to reproduce in a laboratory setting. Note that a material subjected to a frequency of 1 kHz requires nearly 300 hours to accumulate 10^9 cycles. While a component may easily see 300 hours of vibratory loading under steady state conditions, that is a long time under transient conditions typical of many in-service HCF failures.

3. Constant life diagrams

The diagram most widely used for design purposes is a constant life diagram as illustrated in Fig. 2, where available data are plotted as alternating stress versus mean stress for a constant design life, usually 10^7 cycles or higher. This diagram, which can be correctly called a Haigh diagram, is commonly and incorrectly referred to as a Goodman diagram or a Modified Goodman diagram [2]. In the absence of data at a number of values of mean stress, it is often constructed by connecting a straight line from the data point corresponding to fully reversed loading, $R=-1$, with the ultimate tensile strength (UTS) of the material. In some cases (not shown in Fig. 2), the yield stress is the cutoff point on the mean stress axis. Data at $R=-1$ can be obtained readily from a number of techniques using shaker tables to vibrate specimens or components about a zero mean stress, while data at other values of mean stress are often more difficult to obtain, particularly at high frequencies. Alternatives to the straight line approximation in Fig. 2 involve various curves through the yield stress or UTS point on the x-axis, or through actual data if available, to represent the average behavior. Scatter in the data can be handled by statistical analysis which establishes a lower bound for the data. On top of this, a factor of safety for vibratory stress can be included to account for the somewhat indeterminate nature of vibrations, particularly those of a transient type. Finally, design practices or specifications may limit the allowable vibratory stress to be below some established maximum value, independent of the magnitude of the mean stress. The safe life region, considering all of these factors, is shown in Fig. 2. What the shaded region provides, therefore, is an allowable threshold vibratory stress as a function of

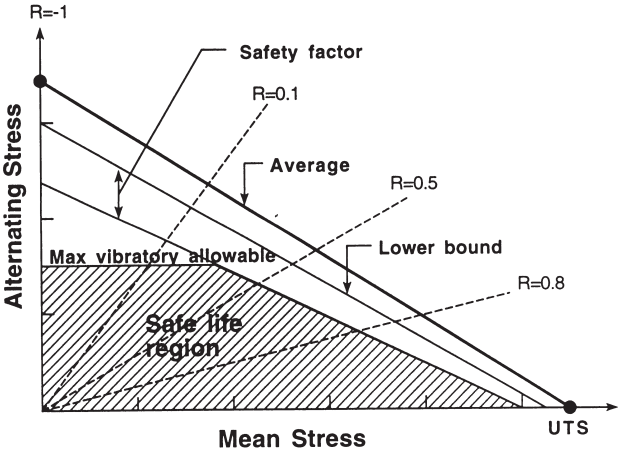

Fig. 2. Schematic representation of a constant life diagram.

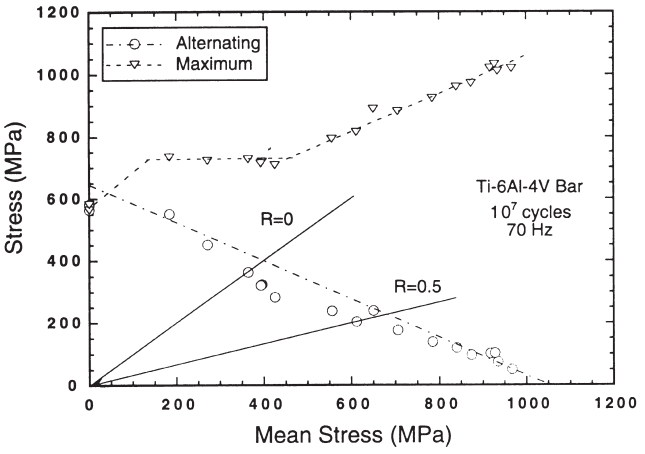

Fig. 3. Haigh diagram for Ti-6Al-4V bar for a life of 10^7 cycles.

mean stress, the latter being fairly well defined because it is closely related to the rotational speed of the engine. If the vibratory stress is maintained within the allowable region on the Haigh diagram, there should be no failure due to HCF and, further, no periodic inspection required for HCF. Provided that the maximum number of vibratory cycles experienced in service does not exceed the number for which the Haigh diagram is established, 10^9 for example, then such a design procedure is one of "infinite" life requiring no periodic inspection.

There are some pitfalls in the use of a Haigh diagram in design, particularly when basing it only on data at $R=-1$. For example, Figs. 3 and 4 show such diagrams for the same material, Ti-6Al-4V, processed into two different product forms, hot rolled bar (Fig. 3), and forged plate (Fig. 4). In addition to the alternating stress, the peak or maximum stress is also shown. The data in Fig. 4 for the plate material are obtained from two independent sources on the same material, shown as ML for my laboratory and ASE for Allied Signal Engines [3]. An unusual feature of the data is the relatively large amount of scatter which occurs under $R=-1$ (fully reversed, zero mean stress) loading. This phenomenon has been observed in several other alloys and is under further investigation. Note also that a straight line does not provide a good representation of the alternating stress data. Note, further, that for high values of mean stress, the maximum stress is quite high, approaching the static ultimate stress of 1030 and 980 MPa for the bar and plate material, respectively. Recent research on fatigue life at high mean stresses [4,5] has shown that at high mean stress, the fracture mode changes from one of fatigue to one of creep. A plot of maximum and minimum stress, Fig. 5, shows the range of vibratory stresses (min. to max.) at each mean stress tested. The stress above which creep occurs is shown along with the line which delineates the region of fatigue, at low mean stresses, from the region of creep, at high mean stresses. Thus, in the creep regime, consideration should be given to the amount of time during which such vibrations occur, not only to the number of cycles. Allowable vibratory stresses, while very low in this region, should also be supplemented with consideration of maximum stresses. It is for these reasons that designers shy away from the high mean stress regime.

4. Damage considerations

While methods appear to be available to quantify the fatigue limit of a material, and to establish a threshold for a crack of an inspectable size, there are still issues remaining over how severe is the damage induced by FOD and fretting fatigue. Other modes of service-induced damage, such as creep, thermo-mechanical fatigue, corrosion, erosion, and initial damage from manufacturing and machining, must also be taken into account in establishing material capability and inspection intervals. The following sections provide a brief description of the issues associated with FOD and fret-

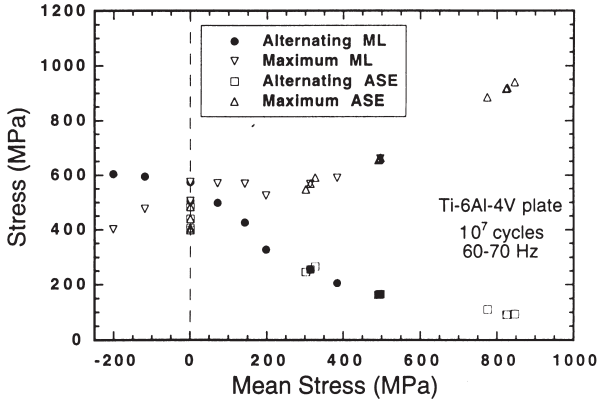

Fig. 4. Haigh diagram for Ti-6Al-4V plate for a life of 10^7 cycles. Data are from Allied Signal Engines (ASE) and Air Force Materials Lab (ML).

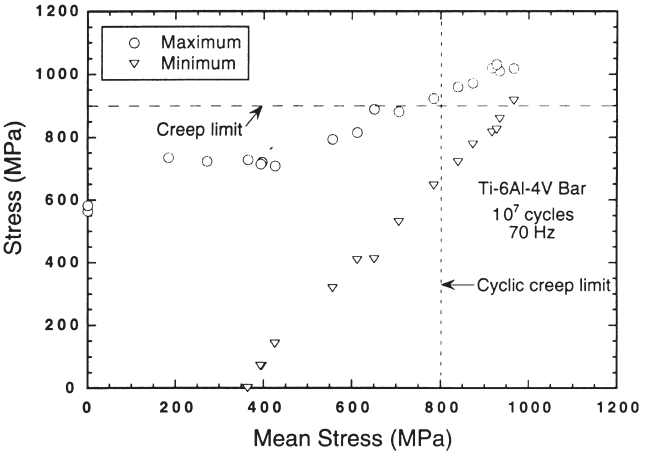

Fig. 5. Haigh diagram showing region of transition in mechanism for high mean stress.

ting. In addition, the role of low cycle fatigue by itself, as well as in conjunction with fretting and FOD, is discussed.

4.1. FOD and notches

Foreign objects impacting leading edges of rotating blades or static structures can produce damage in the form of notches or tears as shown schematically in Fig. 6. Attempts have been made to quantify such damage in the form of an equivalent K_t, but relating that to actual material behavior is difficult. First, it is difficult to establish the effective value of K_t, particularly when residual stresses and permanent deformation are produced ahead of the notch and when small cracks are formed at the tip of the notch. Second, there are an unlimited number of notch geometries involving combinations of depth and radius of notch which will produce the same value of K_t for a given loading condition. Third, while some data exist on the reduction of fatigue life at a given stress due to FOD, there are few data available on the reduction of the fatigue limit, particularly in the very high cycle regime. These "regions of ignorance" are shown schematically in Fig. 6 as dashed lines. Recent work has provided some quantitative results on the fatigue notch factor, K_f (unnotched fatigue limit stress/notched fatigue limit stress) for machined notches in Ti-6Al-4V. Bellows et al. [6] report values of K_f=1.8 and 2.1 for R=−1 and R=0.1, respectively, using specimens with a notch having a K_t=2.5. The fatigue limit is established for 10^7 cycles at 60 Hz. Lanning et al. [7] report values of K_f=2.1, 1.8, and 1.3 for 10^6 cycles for R=0.1, 0.5 and 0.8, respectively, for K_t=2.8 at 50 Hz. These types of data allow design limits for vibratory stress to be established for notches of a known K_t. But how do they relate to the performance of a material which has suffered FOD from a particle impacting at high velocities? Results for values of the fatigue limit in Ti-6Al-4V have recently been obtained using tension specimens which have a leading edge geometry similar to a fan or compressor blade. Tests on a leading edge (LE) specimen whose LE thickness is 0.75 mm (radius 0.38 mm) have been conducted by impacting the LE with 1-mm-diameter glass spheres at a velocity of 300 m/s and at incident angles between 0° and 60° [8]. Results are shown in Fig. 7 which shows the 10^6 cycle fatigue limit for the various conditions normalized with respect to the undamaged material at two values of R. It can be seen that normal incidence, 0° (the angle θ is defined in the figure) is the least damaging for these impacts. The worst condition is when the impact angle is around 30°, although a large amount of scatter is seen in the data. This condition produces fatigue limit stresses which are slightly over half of the smaooth bar values. It is clear that experimental and analytical methods for assessing the extent of FOD damage must consider angle of incidence as an important parameter. It remains to be established whether or not real impact conditions can be simulated in the laboratory without the use of guns to launch projectiles or whether machined notches may provide useful data in assessing the FOD resistance of materials. In addition, damage from real impacts in the form of residual stresses or strains or shear bands must be assessed in order to establish the fatigue limit of the damaged material.

The implementation of data on the FOD resistance into the design process requires steps beyond the establishment of a single equivalent K_t. For example, the geometry of a leading edge of a blade or vane, particularly its thickness, must be considered since FOD resistance due to damage from a given particle will vary with thickness as well as impact angle and velocity. For a probabalistic approach to this problem, consideration must be given either to the types and sizes of particles

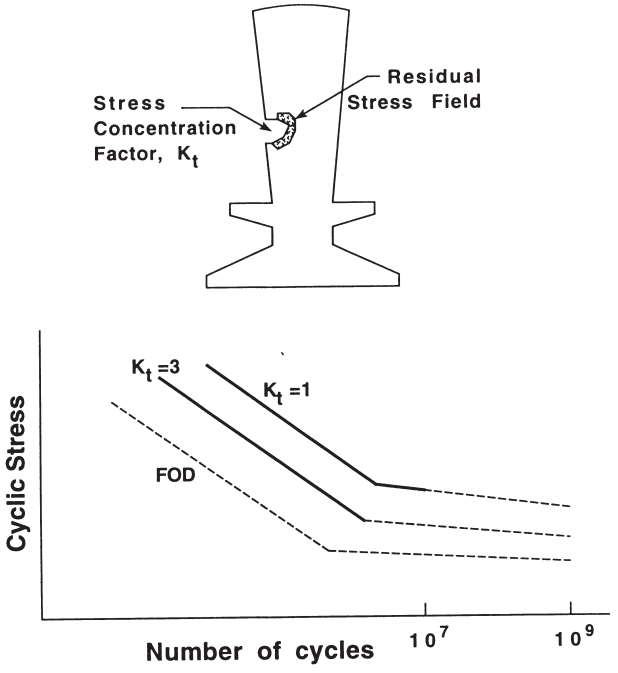

Fig. 6. Schematic of issues and concerns in dealing with fatigue life of material subjected to FOD.

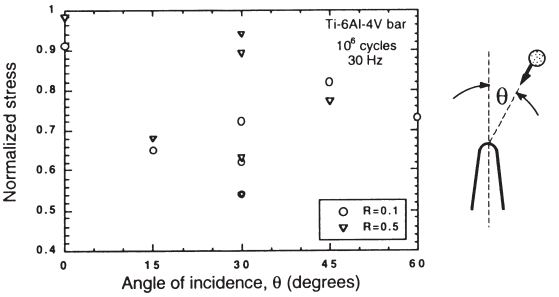

Fig. 7. Effect of incidence angle on normalized fatigue limit for FOD from 1-mm-diameter particles. Normalization is with respect to undamaged material.

which may impact the structure or to the nature of the damage. For the latter, data from field experience are needed but there are few data on the effect of observed damage on the fatigue limit. It would appear that a probabalistic approach to design is needed which combines the probability of an occurrence of FOD at a given location, the extent of the damage, and the probability of vibratory and LCF loading at that location, including an expected number of cycles if the loading is of a transient nature. If a crack propagates due to LCF from a damage zone caused by FOD, the inspectability for such a propagating crack and reliability of that inspection must also be established. In this entire approach, what has to be established is that a crack will not initiate and propagate to failure under HCF alone or in conjunction with LCF loading. The establishment of a fatigue limit or ΔK_{th} for FOD and notches provides the basis for such an approach.

4.2. Fretting

Fretting fatigue in dovetail joints is one of the most difficult and costliest problems in the US Air Force related to HCF. Fretting fatigue occurs when there is relative motion in the contact region between two surfaces. In the two-dimensional schematic of a dovetail, Fig. 8, it is seen that the contact region involves normal and shear loads as well as bending moments across the interface. In addition to the loads shown, there are axial stresses in both the blade and disk in the x–y plane. Further, there are shear contact stresses and resulting axial stresses normal to the plane shown in the figure, i.e. in the z direction. These three-dimensional stresses

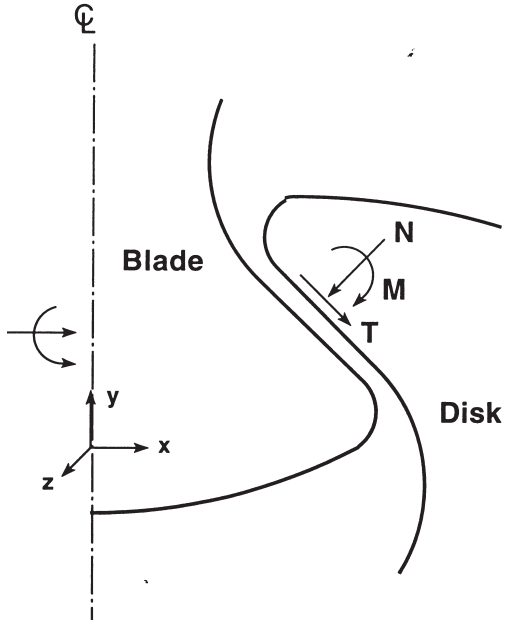

Fig. 8. Schematic of loads in two-dimensional analysis of a dovetail region.

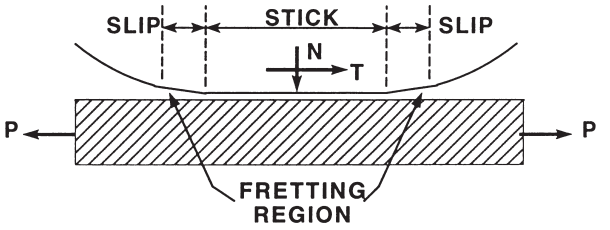

Fig. 9. Schematic of loads and relative motion in contact region under fretting fatigue.

can arise in a component due to a rocking type of vibration about an axis parallel to the x-axis in the figure. Superimposed on the loads from the steady centrifugal loading of the blade are vibratory stresses which can result from blade vibrations. Because of the nature of the stress fields in contact regions, there is always a region of relative slip near the edge of contact, as shown schematically in Fig. 9. The general problem, therefore, involves normal contact forces, N, tangential contact forces, T, axial loading of the material, P, regions of stick and slip, and a relative displacement in the slip region. Depending on the magnitude of this relative motion and the stress fields produced by the steady and vibratory stresses, fretting fatigue can occur near the edges of the contact region. Whether fretting fatigue is due entirely to the relative motion, or whether the complex stress field contributes significantly to the process, is still debated. Nonetheless, laboratory experiments and field usage demonstrate that fretting fatigue can reduce the HCF material capability significantly.

Results for the fatigue limit stress corresponding to 10^7 cycles for specimens held in a fretting pad fixture [9] are presented in Fig. 10. The data shown represent the maximum stress, denoted by "Goodman stress", for tests conducted at two stress ratios using fretting pads with two different radii at the edge of contact. The data are plotted against the average normal (clamping) stress of the pad on the specimen. For comparison purposes,

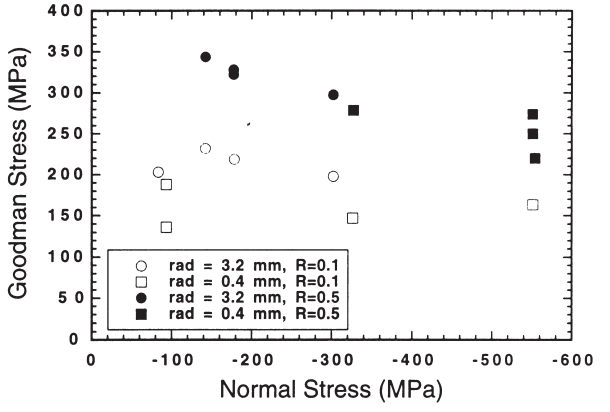

Fig. 10. Fatigue limit stresses (Goodman Stress) under fretting fatigue conditions conditions as a function of the applied normal (clamping) stress.

typical Goodman stress values for the Ti-6Al-4V used as the specimen and pad material are 600 and 825 MPa for R=0.1 and R=0.5, respectively. It can be seen from the figure that the values under fretting conditions are significantly lower than for the unfretted material. To quantify the reduction in fretting capability, an average knockdown factor (KF) is calculated as the unfretted fatigue limit stress divided by the fretting fatigue limit stress. This definition is similar to the one used for notches, K_f. The results are presented in Table 1 and show that the larger contact radius produces the larger value of KF for both values of R=0.1 and 0.5. Second, tests at R=0.1 produce a higher value of KF than those conducted at R=0.5. While these trends and corresponding values of KF are significant and should be taken into account in design, there appears to be no systematic change in Goodman stress with value of clamping stress over the range of clamping stresses which cover roughly a factor of six in this investigation as seen in Fig. 10. The authors conclude tentatively that the normal stress may not have much effect on the relative slip length in the contact region, but clearly more work has to be done to quantify all such effects. These results show, however, that use of a single factor of safety on the allowable alternating stress in a Haigh diagram, a procedure that has been used in design more than once, is not a rational approach and may be non-conservative for some contact stress conditions if the factor of safety is obtained empirically for one specific condition. Note that the values in Table 1 for KF range from 2.6 to 4.2 for the limited range of conditions studied.

A further consideration in developing a rational design methodology for fretting fatigue is the possible extension of a constant life diagram (Haigh or Goodman diagram) to cases where multiaxial stresses occur. In fretting fatigue, the contact region (Fig. 9) will generally involve stresses which can be either tensile or compressive in the part being fretted, a compressive contact stress in a direction normal to the tension or compression in the part, and a shear stress. The multiaxial equivalent of the Haigh diagram (Figs. 3 and 4) might use an effective stress for the alternating stress axis, but when compressive stresses are involved, the effective stress remains a positive number. Shear stress may also be considered as a parameter, but the maximum and minimum shear stresses will generally occur on different planes, so the plane where some combination of these is maximum should probably be used. Finally, if parameters such as shear stress and average pressure (hydrostatic) are used to replace alternating and mean stress, respectively, as the axes in the Haigh diagram, one may find that the points representing this biaxial stress state have no equivalent uniaxial condition which can be obtained in the laboratory. In this case, the multiaxial theory cannot be compared with uniaxial data to see if it is a reasonable representation of the material behavior and the data for the theory have to be generated under multiaxial conditions which are difficult to achieve in the laboratory, particularly in the absence of fretting. There is little experimental work or modeling of material behavior under multiaxial stress states where large compressive stresses are involved such as in the contact region where fretting fatigue occurs.

Table 1
KF values for fretting fatigue

σ_{fret} (MPa)	Radius (mm)	Stress ratio	σ_{ref} (MPa)	KF
144	3.2	0.1	600	4.2
214	0.4	0.1	600	2.8
258	3.2	0.5	825	3.2
323	0.4	0.5	825	2.6

4.3. LCF damage

Design for LCF using damage tolerance insures that LCF cracks will not grow to a catastrophic size during an inspection interval or in the design lifetime of an uninspectable component. It does not insure that a crack of a non-catastrophic size may develop and, only recently, has the potential for that crack growing under HCF been addressed in analysis and design. A simplified engine mission spectrum is shown schematically in Fig. 11 in which the large amplitude cycles represent LCF due to takeoff, landing, and major power excursions, while the small amplitude cycles represent high frequency vibrations superimposed on the dwell portion of the LCF mission profile. The threshold for HCF crack propagation, based on endurance stress, can be altered when going from a undamaged material or component to a damaged component which has a non-catastrophic LCF crack, which is determined from a threshold stress intensity. The same reasoning has to be applied to other damage states such as those due to FOD and fretting. In either case, the damage may be extended initially due to LCF or HCF, depending on the threshold stress intensity corresponding to that damage geometry or state, or

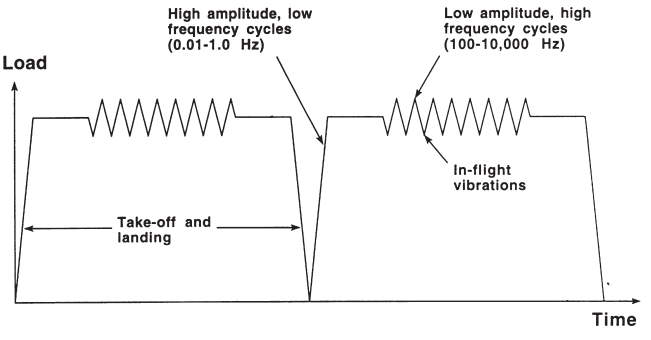

Fig. 11. Schematic of simplified engine mission spectrum.

endurance limit for that same damage. It is thus not sufficient to determine the conditions for the onset of HCF alone. The onset of LCF, which may not produce failure, may extend the damage and reduce the stress or stress intensity for HCF initiation and growth. It is not known for certain at this time whether FOD and fretting are conditions which may lead to failure due to HCF alone, or whether LCF plays a role in the failure process when subsequently combined with HCF. Such issues must be addressed in design and analysis to insure an HCF tolerant component.

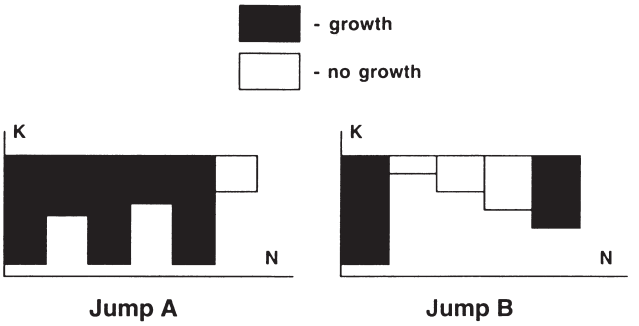

Fig. 13. Schematic of jump loading history [9].

5. HCF damage tolerance

The ultimate goal is to be able to design for HCF in the presence of any type of damage or service usage which degrades the properties of materials under HCF loading. The concept is illustrated in Fig. 12 which shows, schematically, some type of damage which might affect material capability. Such damage state, denoted by D, will have a design life which is some fraction of the actual life under those conditions. The damage may be a continually increasing function, such as LCF, or may be a step function such as FOD. In either case, the material would be removed from service for cause (inspection) or because the design life is reached. For damage from LCF, the material has its least resistance to HCF just prior to removal. For FOD, the degraded properties occur at some point during the service life. These properties may stay constant, as shown, or may further degrade due to another cause such as LCF. A damage tolerant design should address the HCF capability under the most severe and probable damage state, shown schematically in Fig. 12 as the critical damage state. Various approaches to implementing such an approach are discussed in the following sub-sections.

5.1. Crack growth thresholds

For damage in the form of cracks, from FOD, fretting, or LCF, the use of a fracture mechanics threshold to determine the allowable vibratory stress seems to be a promising approach for HCF, and follows the concept now being used successfully for LCF. Provided that an inspection can be made, and crack lengths measured, knowledge of the threshold for crack propagation can be used to assess the susceptibility of the material to HCF crack propagation. If the stresses are maintained below this limit, and the limit corresponds to a sufficiently low growth rate, perhaps 10^{-10} m/cycle or lower, then safe HCF life is assured. The potential growth of such cracks under LCF, and the time interval where such growth produces a crack where HCF might occur, must also be considered. This would establish the required inspection interval. One key issue in this proposed scenario is the determination of a suitable threshold for the types of cracks which may occur in service, some of which could be small enough to be uninspectable with current technology. Various types of loading conditions can be used to determine a threshold, most of which are for long cracks. Lenets and Nicholas [10] used two methods, shown schematically in Fig. 13, where thresholds were obtained from increasing and decreasing ΔK experiments after growing the crack under large amplitude loading. Fig. 14 shows the results which show that the decreasing ΔK threshold (Jump A) is smaller than the increasing ΔK threshold (Jump B). The authors feel that the lower threshold is not realistic because service con-

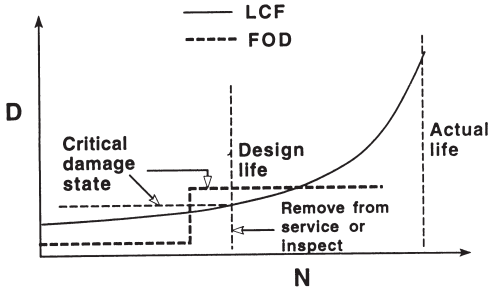

Fig. 12. Schematic of damage accumulation during the life of an engine component.

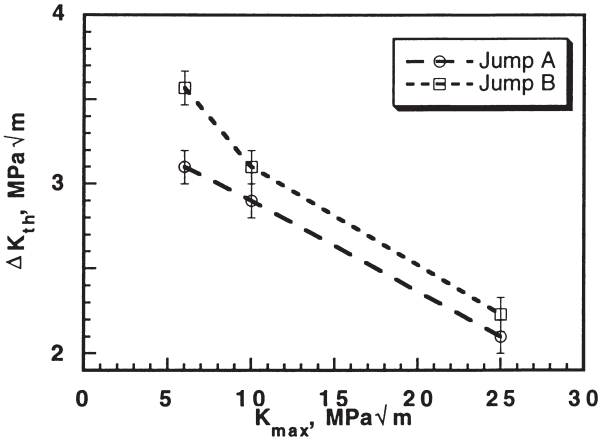

Fig. 14. Threshold data for jump tests [9].

ditions usually produce loadings below threshold until a severe event occurs in which HCF becomes critical, as in Jump B. Boyce et al. [11] conducted tests at 1 kHz frequency and found that a lower bound threshold for small crack propagation could be established from long crack threshold tests at high R under constant-K_{max}/increasing K_{min} conditions. For Ti-6Al-4V, at R=0.92, this lower bound was found to be ΔK=2.2 MPa$\sqrt{m}$ whereas small crack growth behavior from naturally initiated and FOD induced small cracks was not observed below a ΔK of 2.9 MPa$\sqrt{m}$.

The loading history effect illustrated in Figs. 13 and 14 is even more complicated than described above. The number of prior cycles in the Jump B test method, which involves going from a no-growth to a growth condition, affects the threshold value for the onset of crack propagation. At low values of K_{max} (medium to high R) and ΔK only slightly below the ΔK_{th} value, extended cycling applied to the dormant crack tends to decrease the no growth–growth threshold. This observation is attributed to the large number of cycles apparently required to alter the residual stress field ahead of the dormant crack, a process which according to the limited data available takes upward of four million cycles. By contrast, extended cycling with ΔK substantially lower than the ΔK_{th} value applied to the dormant crack (at very high R), tends to increase the FCG threshold. In addition to the residual stress field modification, this result obtained at high K_{max}=25 MPa$\sqrt{m}$, can also be explained by crack blunting via creep or secondary cracking and branching, processes that serve to reduce the effective driving force at the crack tip.

The use of a threshold during a mission cycle becomes even more complicated when each loading sequence can be preceded by an underload or overload of differing magnitude. Such behavior is illustrated in the work of Hawkyard et al. [12] where LCF loading is interspersed with three blocks of HCF loading at different values of R and maximum stress, and where the threshold for each condition is different. It is clear from the experimental data that the threshold for crack extension is dependent on the prior loading sequence. The highest values are found to be from a load shedding test at constant value of R while the lowest values are found from combined HCF/LCF tests where the LCF at low R serves as an underload to the HCF cycles at high R. From these observations, one can conclude that the threshold for fatigue crack propagation depends on the specific test conditions used, whether "standard" or non-standard. It is more important to use a test condition which can be related to service usage than to use a "standard" method which may, in some cases, provide a conservative value of ΔK_{th}.

Of further concern in the establishment of a threshold for crack propagation under HCF conditions is the behavior of small cracks which have been shown to grow at rates exceeding those of long cracks under the same applied stress intensity and to grow at ΔK values below the long crack threshold [13,14]. The small crack "paradox" is often illustrated through the use of a Kitagawa type diagram [15] shown schematically in Fig. 15. On this logarithmic plot of stress against crack length, the long crack threshold is a straight line under the assumption that ΔK is proportional to $\sigma\sqrt{a}$, where σ is the applied stress and a is the crack length. At the same time, the endurance limit stress, σ_e, is a horizontal line. The region below these two lines, not shaded in the figure, is where crack propagation cannot occur because either the stresses are below the endurance limit or the stress intensity is below threshold. In materials with very small cracks, or materials in which there are no cracks, fatigue can take place when the stress is above the endurance limit. It is clear, therefore from the diagram, that the long crack threshold is either not valid for very small cracks or does not have any physical meaning as crack lengths approach zero. Of more concern is the region below the endurance limit where cracks can grow because the stress intensity is above threshold. For long cracks this is to be expected, because the endurance limit does not apply to a material which already has a crack. When this crack becomes very small, a very important consideration becomes how the crack developed. If it occurred during processing of the material, then the endurance limit should be established on material which has these initial defects, because this is the production material which has to be characterized. But many experiments are performed on small cracks where it is shown that small cracks grow at stresses below the endurance limit, and perhaps at stress intensities below the long crack threshold. Such a region is shown as a dashed line in Fig. 15 and is labeled as real materials. The question that has to be raised is how these cracks were formed. It is obvious that they were not initiated under the same loading conditions that they are grown under since the stresses are below the endurance limit. In fact they are routinely initiated under some other type of loading

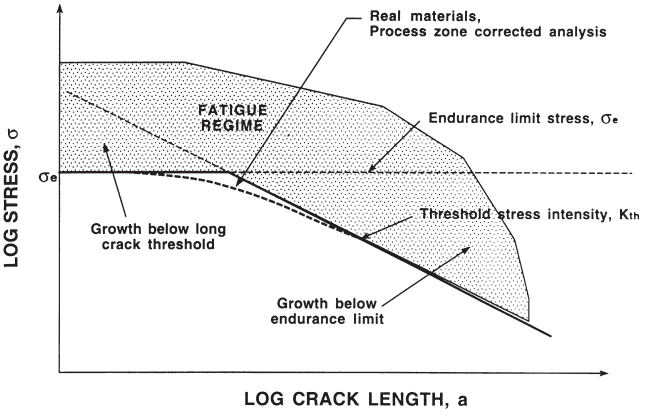

Fig. 15. Kitagawa type diagram.

which can generally be referred to as low cycle fatigue. Once the cracks are present, then a crack growth threshold can be established. What is lost in the process is the load history effect in going from LCF to HCF. Thus, these data represent a LCF/HCF threshold, with little known about the history of loading effect. Note from the discussion above that thresholds determined experimentally for long cracks have values which can depend on the history of loading. The good news in this scenario is that the concern in service applications for the threshold for small crack propagation is only with cracks that were present initially (see discussion above on endurance limit) or ones that form in service. In the latter case, they would have to form by some other (LCF) loading, just as is done in the laboratory. The question that must be answered, therefore, is how the different possible types of LCF loading affect the HCF threshold, and/or whether there is a unique small crack threshold independent of prior loading history.

5.2. Surface treatments

In addition to the implementation of damage tolerance to improve the reliability of HCF design when other damage may occur, procedures are being developed to decrease the materials susceptibility to in-service damage. In addition to shot peening, which improves the fatigue resistance of materials when initiation takes place near the surface, a laser shock peening (LSP) process has been introduced into service to improve the material resistance to FOD. A schematic of the process is shown in Fig. 16 where a pulsed laser impinges on the surface of a material. In actual practice, two pulses impinge simultaneously on both sides of the leading edge of a blade. The rapid ablation of the surface coating generates intense, short duration shock pulses which interfere with each other within the blade and produce a high compressive residual stress at the surface down to depths of the order of nearly 1 mm. Water on the surface acts as a impedance mismatch and serves to constrain the shock pulse within the blade. The compressive residual stresses, which are more intense and much deeper than those developed under conventional shot peening, retard both the initiation and growth of cracks from foreign body impacts or machined notched in the leading edge. An illustration of the benefits of LSP is shown in Fig. 17 where crack length in a three-point bend specimen is shown for various increments of loading [16]. For each load step, the crack grows and then arrests. This happens as the load is increased from 400 to 580 MPa and failure only occurs when a stress of 607 MPa is applied. By contrast, a specimen without LSP fails upon loading at the lowest load level where the crack continues to grow without arrest. The retardation of crack growth for the LSP samples is attributed to the compressive residual stresses which, in turn, provide the equivalent of a superimposed negative K [16].

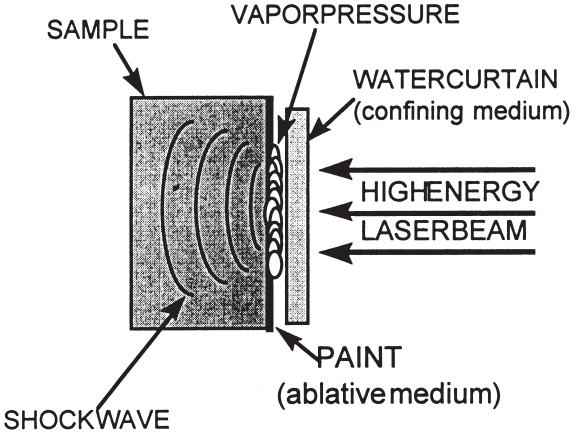

Fig. 16. Schematic of LSP process.

5.3. Margin of safety

A final but not trivial consideration in the development of a damage tolerant approach for HCF is the margin of safety which should be included in the design process. As was pointed out previously, plotting of the maximum stress in a Haigh diagram (see Figs. 3 and 4) shows that the maximum stress is near the yield stress of the material at high values of mean stress. This leaves very little margin for error and, since the allowable alternating stress is small in this region, it forces one to stay away from this region altogether since reducing the allowable alternating stress by a factor of safety would allow essentially no vibratory stress to occur without failure. Another consideration in establishing a margin of safety is the form of the Wohler diagram (S–N curve) as shown schematically for two hypothetical materials in Fig. 18. As drawn, the two materials have the same value of the fatigue limit corresponding to 10^7 cycles, but the S–N behavior is different for the lower cycle regime. If a design were based strictly on the Haigh diagram corresponding to 10^7 cycles, then the two materials would be designed for identical allowable vibratory stresses. Note, however, that if during a period of transi-

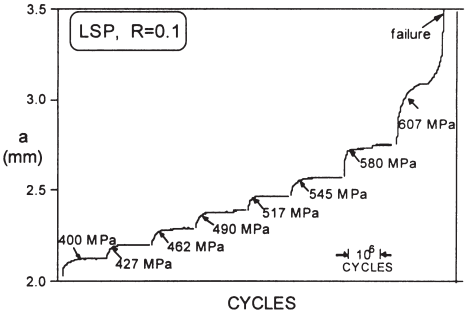

Fig. 17. Sample LSP crack growth data.

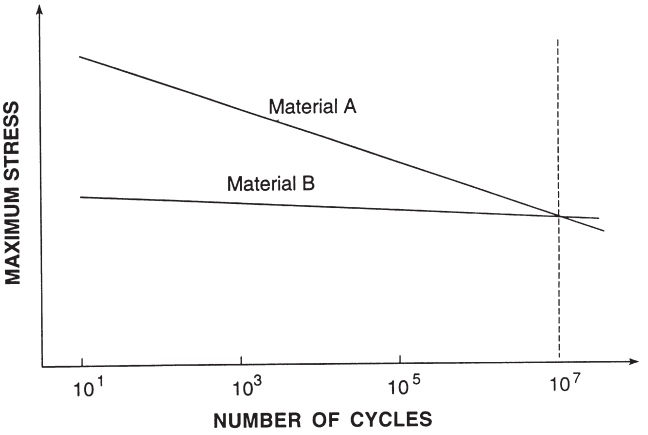

Fig. 18. Wohler diagram for two materials.

ent vibration the 10^7 cycles allowable stress were to be exceeded for a short period of time, Material A would be able to accommodate such stresses for a limited number of cycles while Material B would have no such capability. Methods should be developed to include this consideration in the design process, just as ductility or fracture toughness are often not part of the design procedure but higher values make one feel better about the material capability. A similar argument to that comparing the materials in Fig. 18 can be made when considering the *S–N* behavior of the same material at different values of stress ratio, *R*, as shown in Fig. 19 for Ti-6Al-4V. At low values of *R*, there seems to be some capability for this material to sustain a limited number of cycles above the 10^7 cycles fatigue limit whereas at R=0.8, there is no tolerance for even a limited number of cycles above the fatigue limit. As noted previously, the fatigue limit at this high value of *R* is near the static ultimate stress of the material (980 MPa), so there is little tolerance for overstressing the material. These concerns help explain why design practice has to avoid operational conditions which subject the material to vibratory stresses in the high *R* regime. It is also of interest to note that the knee in the *S–N* plots, Fig. 19, occurs at increasing cycle count as stress ratio is increased from $R=-1$ to R=0.8 based on an eyeball approximation of a bilinear fit to the data. This observation serves to point out that care must be exercised when choosing the number of cycles corresponding to a fatigue limit if this is also going to be used as an engineering estimate of the endurance limit. In fact, some recent data have shown that no endurance limit exists for lifetimes exceeding 10^9 cycles in some materials [17].

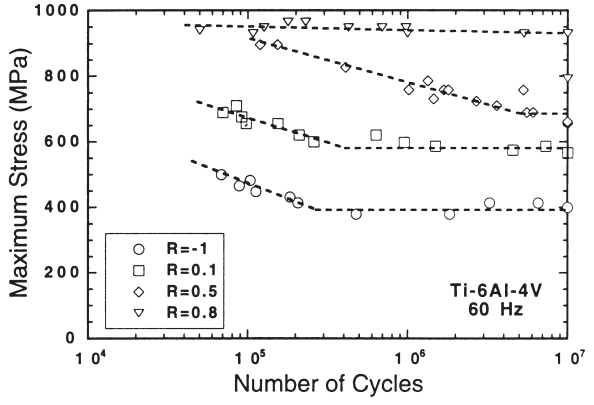

Fig. 19. Wohler diagram for Ti-6Al-4V at 60 Hz.

6. Concluding remarks

Damage tolerant approaches for HCF are still in the development stage. Whatever their final form, it seems clear that they will involve the use of a threshold concept, a criterion for a smooth or damaged material below which HCF will not occur. The criterion could be in the form of a stress or a stress intensity. From a maintenance and life extension point of view, it is important to be able to quantify the level of damage that may be present from other than HCF, such as from LCF, FOD, or fretting. This may be accomplished by inspection, analysis, probabilistics, or some combination of these. In addition, methods need to be established to predict the growth or extension of any such damage so that material capability limits are not exceeded before the next inspection or the component is removed from service.

It should also be noted that most of the discussion in this paper dealt with material behavior in a deterministic manner. The use of minimum material capability in design, as illustrated in the Haigh diagram of Fig. 2, may result in ultra conservative estimates of the probability of failure or may be conservative in estimating allowable vibratory stresses. A probabalistic approach to HCF design based on statistics of loading functions, structural response, material capability and probability of damage, and their synergism, may be the most rational manner to arrive at design allowable.

Acknowledgements

This work was conducted at the Air Force Research Laboratory, Materials and Manufacturing Directorate, under the National Turbine Engine High Cycle Fatigue Program. The author would like to thank his colleague, Dr. George Sendeckyj, for many stimulating discussions and comments.

References

[1] Engine Structural Integrity Program (ENSIP), MIL-STD-1783 (USAF), 30 November 1984.
[2] Sendeckyj GP. History of constant life diagrams. In: Srivatsan

TS, Soboyejo WO, editors. High cycle fatigue of structural materials. TMS, 1998:95–107.
[3] Bellows RS, Muju S, Nicholas T. Validation of the step test method for generating Haigh diagrams for Ti-6Al-4V. Int J Fatigue 1999;21(7):687–97.
[4] Morrissey RJ, McDowell DL, Nicholas T. Frequency and stress ratio effects in high cycle fatigue of Ti-6Al-4V. Int J Fatigue 1999;21(7):679–85.
[5] Morrissey RJ. Frequency and mean stress effects in high cycle fatigue of Ti-6Al-4V. WL-TR-97-4100, Wright-Patterson AFB, OH, 1997.
[6] Bellows RS, Bain KR, Sheldon JW. Effect of step testing and notches on the endurance limit of Ti-6Al-4V. In: Davis DC et al., editor. Mechanical behavior of advanced materials, MD-vol. 84. New York: ASME, 1998:27–32.
[7] Lanning D, Haritos GK, Nicholas T. Notch size effects in HCF behavior of Ti-6Al-4V. Int J Fatigue 1999;21(7):643–52.
[8] Ruschau J, Thompson S, Nicholas T. Effects of simulated FOD on fatigue strength of Ti-6Al-4V. Paper presented at 4th National Turbine Engine High Cycle Fatigue Conference, Monterey (CA), 9–11 February 1999.
[9] Hutson A, Nicholas T, Goodman R. Fretting fatigue of Ti-6Al-4V under flat on flat contact. Int J Fatigue 1999;21(7):663–9.
[10] Lenets YN, Nicholas T. Load history dependence of fatigue crack growth thresholds for a Ti-alloy. Eng Fract Mech 1998;60:187–203.
[11] Boyce BL et al. Thresholds for high-cycle fatigue in a turbine engine Ti-6Al-4V alloy. Int J Fatigue 1999;21(7):653–62.
[12] Hawkyard M, Powell BE, Stephenson JM, McElhone M. Fatigue crack growth from simulated flight cycles involving superimposed vibrations. Int J Fatigue 1999;21(S2):S59–68.
[13] Miller KJ. The short crack problem. Fatigue Eng Mater Struct 1982;5:223–32.
[14] Ritchie RO, Lankford J, editors. Small fatigue cracks. Warrendale (PA): The Metallurgical Society, 1986.
[15] Kitagawa H, Takahashi S. Applicability of fracture mechanics to very small cracks or the cracks in the early stage. In: Proceedings of 2nd International Conference on Mechanical Behaviour of Materials, Boston (MA), 1976:627–31.
[16] Ruschau JJ, John R, Thompson SR, Nicholas T. Fatigue crack growth rate characteristics of laser shock peened titanium. ASME J Eng Mater Tech 1999;121:321–9.
[17] Nishijima S, Kanazawa K. Stepwise S–N curve and fish-eye failure in Giga cycle fatigue. Conference on Fatigue in the Gigacycle Regime, Paris (France), June 1998.